OPTICAL–OPTICAL DOUBLE RESONANCE ON COOLED MOLECULAR IONS: ROTATIONAL ASSIGNMENTS IN THE PERTURBED CO_2^+ $\tilde{B}$–$\tilde{X}$ SYSTEM

Mark A. JOHNSON, Joelle ROSTAS ‡ and Richard N. ZARE ‡
Department of Chemistry, Stanford University, Stanford, California 94305, USA

Received 4 August 1982, in final form 23 August 1982

Population labeling optical–optical double resonance has been applied to CO_2^+ cooled in a supersonic expansion to study the highly perturbed $\tilde{B}(000)$–$\tilde{X}(000)$ band (2900 Å). Three interacting vibronic levels are found and followed to their origins.

1. Introduction

About seven years ago population labeling optical–optical double resonance (PLOODR) was suggested as a means for analyzing electronic transitions [1], but only within the past three years has the promise of this technique been realized for complex molecular spectra. In particular, selected bands of Cs_2 [2] and NO_2 [3,4] were unambiguously assigned by combining OODR with polarization spectroscopy in relatively high pressure bulb experiments (0.1–1.0 Torr). In each case, the lower level labeling technique allowed perturbations in the upper electronic state to be systematically unraveled. In order to isolate individual rotational transitions in highly congested bands of NO_2 [5] and BaI [6], it was necessary to apply PLOODR to the Doppler-reduced spectra afforded by collimated molecular beams. The successful application of PLOODR to the BaI radical at beam densities emphasizes the sensitivity of this method when the lower level label is monitored with laser excited fluorescence. In this work we report an application of PLOODR where its high sensitivity and spectral simplification capability are demonstrated in one of the most demanding areas of molecular spectroscopy: molecular ions. The $\tilde{B}\,^2\Sigma_u^+(000)$–$\tilde{X}\,^2\Pi_g(000)$ band of CO_2^+ presents an outstanding candidate for this demonstration. Its 2900 Å spectrum (fig. 1) is complicated by intramolecular perturbations in the $\tilde{B}\,^2\Sigma_u^+(000)$ state and is characterized by irregular rotational structure, extra lines, and anomalous intensities. As a result, the spectrum has frustrated unambiguous rotational assignment since the first high-resolution spectrum was obtained in 1941 [7]. Ubiquitous weak and extra lines at low J, overlapped by high J members of other branches, have precluded analysis. Indeed, the number of interacting vibronic levels was uncertain, although the $\tilde{A}\,^2\Pi_u$ state has been shown to be responsible for these perturbations [8].

As illustrated in fig. 1, the regions around 2883 and 2884.5 Å are sufficiently congested that combination difference methods fail because of the plethora of blended lines, even at Doppler-limited resolution (0.1 cm^{-1}) in laser excitation spectroscopy (expanded region of fig. 1). Very recently, Rostas and Tuckett [9] reported the emission spectrum of CO_2^+ cooled in a supersonic jet. This work has cleared up some of these low J assignments. However, sequence overlap from $\tilde{B}(100)$–$\tilde{X}(100)$ and the use of moderate resolution (0.2 cm^{-1}) still resulted in a blending of lines, causing assignment uncertainties in the central 2884 Å region.

In our approach to this problem, we draw on two spectroscopic techniques which have been extended to the study of molecular ions: supersonic expansion

‡ Laboratoire de Photophysique Moléculaire du CNRS, Associé à l'Université de Paris-Sud, Bâtiment 213, Université de Paris-Sud, 91405 Orsay Cedex, France.

‡ Holder of a Shell Distinguished Chair, funded by the Shell Companies Foundation, Inc.

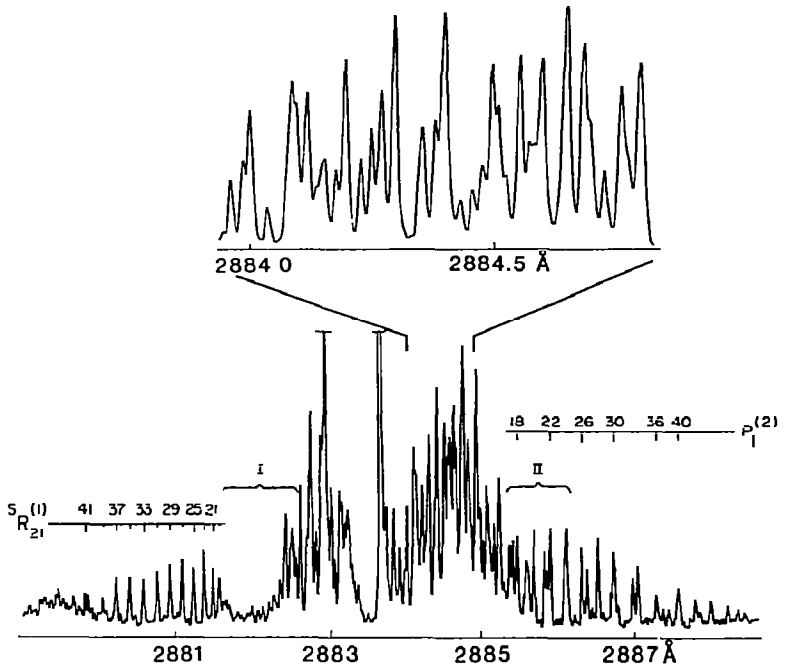

Fig 1 Survey excitation spectra of the region around the $\tilde{B}\,^2\Sigma_u^+(000)$–$\tilde{X}\,^2\Pi_{g3/2}(000)$ sub-band of (thermal) CO_2^+. The expanded section is obtained by pressure scanning the laser ($\Delta\nu = 0.09\ cm^{-1}$). The superscripts on the branch designations are defined in the text.

cooling [10,11] and double resonance [12,13]. Initially, we coupled the spectral simplification obtainable from expansion cooling with high-resolution laser excitation spectroscopy. This yielded accurate ($\pm 0.02\ cm^{-1}$) measurements of low J line positions (see for example fig. 2). However, even this technique, which is free of $\tilde{B}(100)$–$\tilde{X}(100)$ overlap, failed to permit assignment of many lines because the perturbed nature of the spectrum does not allow recognition of the branch structure. To overcome this problem, we then applied PLOODR to jet-cooled CO_2^+. The lower level quantum numbers for 29 of the total number of lines ($\approx$90) were determined. This information so constrains the possible transitions that a unique assignment is readily achieved without the need to recognize the branch structure pattern. In this way we have identified three interacting vibronic states as the cause of the complex appearance of the $\tilde{B}(000)$–$\tilde{X}(000)$ band. Moreover, we have followed *both* parity components of the three vibronic states to their origins.

2. Experimental

The essential features of the PLOODR experiment have been reviewed elsewhere [14]. In the version of this method employed here, two pulsed dye lasers are used: a weak probe laser and a powerful pump laser. The probe laser is fixed on an unknown line in the (2900 Å) $\tilde{B}(000)$–$\tilde{X}(000)$ spectrum and the population in the lower level of this transition is monitored by detecting the resulting fluorescence. The pump or saturating laser is then scanned through the known $\tilde{A}(202)$–$\tilde{X}(000)$ system (2776 Å). When both lasers excite a common lower level, population driven out of the level by the pump laser is observed as a depletion in the fluorescence signal generated by the probe and thus assigns the lower level quantum number in the probe transition. Note that the time between the pump and probe laser pulses must be sufficiently short that the labeled molecules are still confined to the region defined by the diameter of the pump beam and that collisional repopulation is unimportant. The branch assignment is achieved by using known ground-

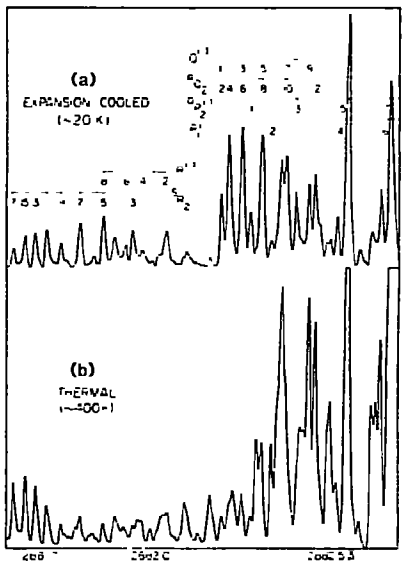

Fig. 2. Expanded excitation spectrum of region I of fig. 1 which corresponds to the vicinity of the upper vibronic origin (see fig. (a) Excitation spectrum from rotationally cooled CO_2^+, a (b) same scan from thermal CO_2^+. The assignments given result from analysis of the PLOODR data.

state combination differences [15] in conjunction with the line positions obtained by high-resolution laser excitation spectroscopy.

The experimental procedure is based on the pulsed laser-induced fluorescence (LIF) method described by Allison et al. [16], modified by the addition of a CO_2 molecular beam and Nd : YAG pumped dye laser. A rotationally cold (≈20 K) molecular beam of CO_2 is formed by expanding 1.0 atm CO_2 through a 0.1 mm glass nozzle. An electron beam is pulsed on for 100 μs to generate rotationally cold CO_2^+ by electron impact ionization of the CO_2 beam. The pump laser (Quanta-Ray Nd : YAG pumped dye laser, frequency doubled to obtain 3 5 mJ/shot at 0.3 cm^{-1} bandwidth) is then fired 1.0 μs after the electron beam is switched off, and the resulting LIF collected with a photomultiplier (PMT) and boxcar averager (PAR 162). Next, 1.5 μs after the pump laser, the probe laser (Molectron N_2-pumped dye laser, frequency doubled to obtain 20 μJ/shot at 0.09 cm^{-1} bandwidth) is passed through the CO_2^+ cloud, and again the resulting LIF detected with a boxcar. Note that the fluorescence lifetimes for the excited states of CO_2^+ are rather short ($\lesssim$ 160 ns) [17–19] so that the LIF from the high-power pump laser does not interfere with the detection of the probe laser LIF. Both beams are softly focused to a diameter of 3 mm at the interaction region, located 13 mm from the nozzle. Each dye laser is operated in an oscillator–amplifier configuration. The output of both oscillators is narrowed by the addition of an intracavity etalon, and scanned by pressure tuning the oscillators with SF_6. The probe LIF, after being integrated by the boxcar, is stored in a signal averager (Nicolet 1170) so that repetitive scans may be co-added to improve the signal-to-noise ratio. The fundamental frequency from the nitrogen-pumped dye laser is split off from the doubled beam and passed through an iodine cell for wavelength calibration [20]. The line positions in the $\tilde{B}$–$\tilde{X}$ region used in this study are reproducible to 0.02 cm^{-1} and consistent within this error with previous determinations [21], where comparisons can be made.

3. Results

Typical double resonance spectra from the jet are presented in fig. 3 along with the relevant energy level diagram. Fig. 3a displays the behavior of the LIF from the probe laser as the pump laser is scanned. The probe laser is fixed at 34681.30 cm^{-1} on one of the $R_1(4.5)$ lines of the $\tilde{B}\,^2\Sigma_u^+(000)$–$\tilde{X}\,^2\Pi_{g\,3/2}(000)$ band Fig. 3b results from detection of the LIF due to the pump laser as it is scanned through the $\tilde{A}\,^2\Pi_{u\,3/2}(202)$–$\tilde{X}\,^2\Pi_{g\,3/2}(000)$ band. As discussed previously, a dip appears in the upper trace when both lasers excite transitions with a common lower level. (The analysis of the previously unknown $\tilde{A}(202)$–$\tilde{X}(000)$ band was itself verified using OODR and will be reported later.) Thus, dips appear as the pump laser excites the $P_1(4.5)$, $Q_1(4.5)$, and $R_1(4.5)$ transitions (see fig. 3c), assigning the lower level of the transition excited by the probe laser. Note that substantial population depletion is observed (≈40%) and that the width of the dips (≈1 cm^{-1}) is undoubtedly due to saturation caused by the pump laser lineshape (sharp feature of 0.3 cm^{-1} on a broad pedestal of 1.0 cm^{-1}). The spectrum shown in fig. 3b was recorded at much reduced laser power (10X) than that used to generate the dips in fig. 3a.

This double resonance procedure was applied to 29

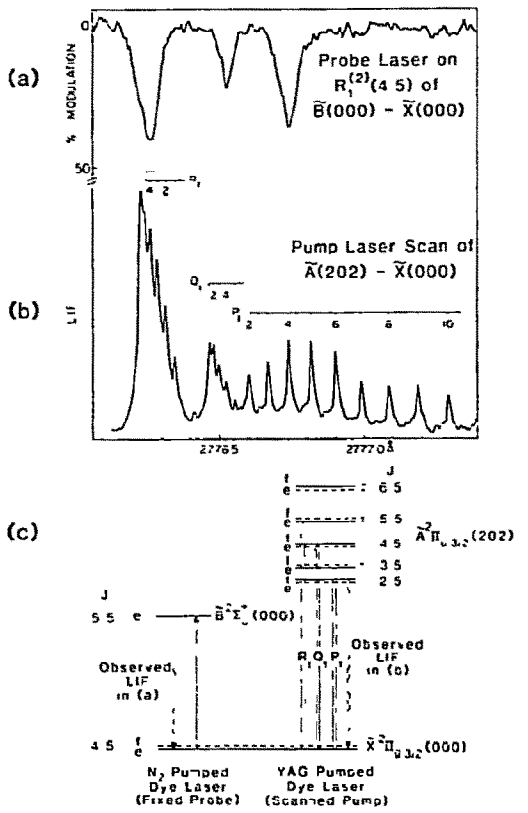

Fig. 3. Population labeling optical–optical double resonance: (a) LIF signal from the probe laser (N_2-pumped dye) fixed at 34681.30 cm^{-1} on the $R_1^{(2)}(4\,5)$ transition of the $\tilde{B}\,^2\Sigma_u^+(000)$–$\tilde{X}\,^2\Pi_{g\,3/2}(000)$ sub-band as the pump laser is scanned (average of three scans); (b) excitation spectrum from the pump laser (Nd : YAG-pumped dye) scanning the $\tilde{A}\,^2\Pi_{u\,3/2}(202)$–$\tilde{X}\,^2\Pi_{g\,3/2}(000)$ sub-band; (c) level diagram indicating the origin of the transitions observed in (a).

of the 90 strong transitions observed in the $\tilde{B}\,^2\Sigma_u^+(000)$–$\tilde{X}\,^2\Pi_{g\,3/2}(000)$ excitation spectrum of cooled CO_2^+. Fifteen additional lines were checked by OODR in the thermal (≈400 K) beam–gas arrangement to verify and extend to higher rotational quantum numbers extra e parity levels found by Rostas and Tuckett [9]. The lower level quantum numbers, line positions, and branch assignments are given in table 1. Note that some of the lines are blends and therefore two lower levels are found in the double resonance experiment. The superscript on the branch notation, e.g. $^SR_{21}^{(1)}$, serves to distinguish branches originating from the three different vibronic bands, with (1) referring to the upper, (2) the middle, and (3) the lower levels.

The results of the double resonance experiment are presented in the form of a reduced term value plot in fig. 4. The most striking features of fig. 4 is the clear evidence of three vibronic origins near the previously estimated position of the $\tilde{B}(000)$–$\tilde{X}(000)$ origin at 34598 cm^{-1} [21]. The upper origin at 34615 cm^{-1} is observed here for the first time, as are the f parity levels of the lower state at 34589 cm^{-1}. The e parity levels of the middle state were also observed by Rostas and Tuckett [9], but the low J transitions used were incorrectly assigned, presumably owing to moderate resolution, sequence overlap from $\tilde{B}(100)$–$\tilde{X}(100)$, and the signal-to-noise obtainable in their study. The e levels of the lower state, first found by these authors, are verified to be correct in this work.

As an indication of the difficulty facing previous workers in finding these extra origins, we have recorded high-resolution spectra in the region around 34615 cm^{-1} (region I in fig. 1) corresponding to the origin of the upper levels in fig. 4. Fig. 2a is a spectrum from the jet CO_2^+ source while fig. 2b was obtained from thermal CO_2^+ (400 K). Comparison of figs. 2a and 2b shows that, even at Doppler-limited resolution in the thermal spectrum, these low J lines are well disguised by overlap with high J members from other rotational branches. The $^SR_{21}^{(1)}$ branch assignments are substantially different than those presented in ref. [21], and these new assignments play a crucial role in the assignment of the perturbing state [22]. Identification of the high J transitions derived from the lower e levels also resolves a problem regarding the nature of a progression of doublets observed to accompany the $P_1^{(2)}$ branch, seen in the low-resolution scan in fig. 1 (region II). These doublets are actually caused by the accidental overlap of the $Q_1^{(3)}$ and $P_1^{(3)}$ branches (see table 1).

4. Discussion

The term values displayed in fig. 4 provide the first complete description of the perturbations at play in the $^{12}CO_2^+\,\tilde{B}\,^2\Sigma_u^+(000)$ level. Previous attempts to analyze in emission the $CO_2^+\,\tilde{B}$–$\tilde{X}$ origin band at 2900 Å failed due to the complexity of the spectrum result-

Table 1
Summary of line positions, lower level quantum numbers obtained by double resonance, and branch assignments for the $\tilde{B}\,^2\Sigma_u^+(000)-\tilde{X}\,^2\Pi_{g\,3/2}(000)$ sub-band of CO_2^+

	ν	J''	Branch
rotationally cooled CO_2^+	34702.56	17.5	$S_{R_{21}^{(1)}}$
	2.13	15.5	$S_{R_{21}^{(1)}}$
	1.77	13.5	$S_{R_{21}^{(1)}}$
	1.35	11.5	$S_{R_{21}^{(1)}}$
	695.00	4 5	$R_{Q_{21}^{(1)}}$
	94 51	6 5	$R_{Q_{21}^{(1)}}$
	93 83	8 5,5.5	$R_{Q_{21}^{(1)}}, Q_1^{(1)}$
	84.69	7 5	$S_{R_{21}^{(2)}}$
	81.96	3.5,6 5	$S_{R_{21}^{(2)}}, R_1^{(2)}$
	81.30	4 5	$R_1^{(2)}$
	80 46	2.5(1 5?)	$R_1^{(2)}, S_{R_{21}^{(2)}}$
	78.52	4.5	$R_{Q_{21}^{(2)}}$
	77 76	3.5	$Q_1^{(2)}$
	77 12	5 5	$Q_1^{(2)}$
	76 90	7 5	$S_{R_{21}^{(3)}}$
	76.32	7.5,2 5	$Q_1^{(2)}, P_1^{(2)}$
	75.93	3.5	$Q_{P_{21}^{(2)}}$
	75.69	5 5	$S_{R_{21}^{(3)}}$
	75.29	4.5	?
	74 33	5.5,4.5	$Q_{P_{21}^{(2)}}, P_1^{(2)}$
	74.16	3.5	$S_{R_{21}^{(3)}}$
	72.69	7.5,8.5	$Q_{P_{21}^{(2)}}, R_1^{(3)}$
	72.25	6.5	$P_1^{(2)}, R_1^{(3)}$
	71.70	4.5	$R_1^{(3)}$
	71 01	2 5	$R_1^{(3)}$
	70 78	4.5,6.5	$R_{Q_{21}^{(3)}}, R_{Q_{21}^{(3)}}$
	70.50	2 5,8.5	$R_{Q_{21}^{(3)}}, R_{Q_{21}^{(3)}}$
	67 53	5.5	$Q_1^{(3)}$
	66.59	5 5,7.5	$Q_{P_{21}^{(3)}}, Q_1^{(3)}$
thermal CO_2^+	34660 19	8.5	$P_1^{(3)}$
	59.42	17.5	$Q_1^{(3)}$
	57 62	10.5	$P_1^{(3)}$
	57.18	19 5	$Q_1^{(3)}$
	55 37	25.5	?
	54.90	12.5	$P_1^{(3)}$
	54 57	21.5	$Q_1^{(3)}$

Table 1 (continued)

ν	J''	Branch
51 96	14 5	$P_1^{(3)}$
51 62	23.5	$Q_1^{(3)}$
48 82	16.5	$P_1^{(3)}$
48 53	24 5	$P_1^{(2)}$
48 29	25 5	$Q_1^{(3)}$
45 40	18.5	$P_1^{(3)}$
41.60	20 5	$P_1^{(3)}$
37 49	22 5	$P_1^{(3)}$

ing from numerous extra lines and from sequence overlap. Pairs of main and extra lines have been observed in the $\tilde{B}$–$\tilde{X}$ origin region, but the system could not be deperturbed with a two-level model [21]. This led to the suggestion that the $\tilde{B}(000)$ level was involved in simultaneous interaction with two or more vibronic levels. If this were the case, the original oscillator strength in a single $\tilde{B}(000)$–$\tilde{X}(000)$ rotational transition would be split into three or more components. Tuckett and Rostas [9] found the e parity frag-

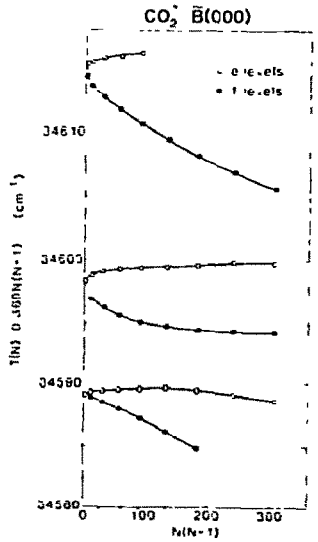

Fig. 4. Reduced term value plot of observed levels in the 34600 cm^{-1} region. The coefficient (0.369 cm^{-1}) is arbitrary and chosen for convenience in displaying the data.

ment of a state roughly 10 cm^{-1} below the energy traditionally regarded as the $\widetilde{B}$–$\widetilde{X}$ origin, but in no case had all three levels of a given parity been located. Thus, the significance of this work lies in the observation of both parity components of three interacting states down to their respective origins.

The fluorescence intensity in the 3000–4500 Å region varies markedly with rotational level when the $\widetilde{B}(000)$–$\widetilde{X}(000)$ band is excited at 2900 Å [8]. This rotational dependence identifies the perturber as the $\widetilde{A}\,^2\Pi_u$ state, since levels composed mostly of $\widetilde{A}$ state character fluoresce primarily in the 3000–4500 Å region, while unperturbed levels are constrained by vibrational overlap to fluoresce in the 2900 Å region. The results of such a study [22] indicate that both upper vibronic levels are derived from the $\widetilde{A}\,^2\Pi_u$ state. They are excited in the 2900 Å region through intensity borrowing from the $\widetilde{B}\,^2\Sigma_u^+(000)$ level. This mixing accounts for the fact that the upper state could not be detected in emission, even with a jet-cooled CO_2^+ source, since most of the emission from these levels occurs over many sequence bands in the 3000–4500 Å region. On the other hand, the use of excitation spectroscopy permits the observation of these levels since all fluorescence from an upper level is detected essentially independently of its spectral distribution.

The shapes of the reduced term value plots in fig. 4 provide insight into the nature of these perturbing states. The rotational energy of states that are well characterized by Hund's case b show a linear dependence on $N(N+1)$, with the e and f components of a particular N level close in energy compared to the spacing between successive N levels. Such a situation is displayed by the lower set of levels in fig. 4 near the origin. It is interesting to note that laser-excited fluorescence studies [8] indicate that the lower state has primarily $\widetilde{B}\,^2\Sigma_u^+(000)$ character for low J levels, consistent with case b behavior in a $K = 0$ state ($K = \Lambda + l$ where l is the vibrational angular momentum quantum number). In the upper state at 34615 cm^{-1}, however, the e and f parity levels do not appear to be derived from the spin splitting of a common N level, but are more consistent with Hund's case a behavior. This evidence suggests that the upper term values correlate to a vibronic state with $K = \pm 1$ symmetry. Both e and f term values for this state form straight lines when plotted versus $J(J+1)$, further supporting the $K = \pm 1$ identification. Since the $J = 1/2$ level is observed for the upper states it likely corresponds to the $^2\Pi_{1/2}$ component of a $^2\Pi$ state. For the middle levels, the case is not obvious. Caution must be exercised here in overinterpreting these observations as the unperturbed vibronic origins of the middle and lower levels are probably quasi-degenerate, so that these levels are interacting primarily at low J. Therefore, the unperturbed shape of the term value plot can be substantially different from that observed. The positions of the vibronic origins are, however, quite well defined and this information puts rigid constraints on the possible vibrational quantum numbers of the perturbers. In particular, both perturbing states must involve several quanta of the bending vibration since it is known [23] that no combination of ν_1 and ν_3 is calculated to lie in this region. This activity of the bending vibration creates another difficulty in interpreting the term value plot since the rotational structure of the perturbing states will be complicated by the Renner–Teller effect in the linear $\widetilde{A}\,^2\Pi_u$ state. The question of the electronic parentage of the three vibronic states found in this work will be elaborated later [22].

Finally, it is instructive to cast the CO_2^+ interelectronic coupling problem in the language of radiationless transitions [24]. The perturbations observed in this linear triatomic system occur on a higher level of complexity than those observed in diatomic molecules, as many vibronic levels of the $\widetilde{A}$ state are close to the $\widetilde{B}(000)$ level and can interact [25]. For instance, the $\widetilde{A}(022)$ state, calculated to lie in this region, has itself four $K = 1$ components. Additionally, these $\widetilde{A}$ state vibronic levels are mixed by anharmonic and Fermi-type interactions. As a result, CO_2^+ displays the first signs of an "internal conversion" process on a spectroscopic level, where the oscillator strength to one electronic state ($\widetilde{B}\,^2\Sigma_u^+$) is being broken into many components by interaction with several vibronic components of another electronic state ($\widetilde{A}\,^2\Pi_u$). The system behaves as if energy pumped into the $\widetilde{B}(000)$ state is channeled to the $\widetilde{A}$ state vibronic manifold, while we are in fact always exciting single eigenstates. Thus CO_2^+ provides a model system in which the mixed-character properties of the individual states can be probed at a step intermediate between the simple diatomic and the dense polyatomic cases.

Acknowledgement

Advice on the expansion cooling technique from J.P. Maier and D. Klapstein and the use of equipment from the San Francisco Laser Center is gratefully acknowledged. We thank R.P. Tuckett for making available to us information prior to publication. This work was supported in part by the Air Force Office of Scientific Research under AFOSR 81-0053-A and by the National Science Foundation foreign travel grant NSF INT TRAVEL 79-24367.

References

[1] M.E. Kaminsky, R.T. Hawkins, F.V. Kowalski and A.L. Schawlow, Phys. Rev. Letters 36 (1976) 671.
[2] M. Raab, G. Honing, W. Demtröder and C.R. Vidal, J. Chem. Phys. 76 (1982) 4370.
[3] R.E Teets, N.W. Carlson and A L Schawlow, J. Mol. Spectry. 78 (1979) 415
[4] J C D Brand, K J Cross and N P Ernsting, Chem Phys 59 (1981) 405,
J.C.D. Brand and N.P. Ernsting, J Mol. Spectry. 91 (1982) 389.
[5] W. Demtröder, D. Eisel, H.J. Foth, G Honing, M. Raab, H.J. Vedder and D. Zevgolis, J. Mol. Struct 59 (1980) 291.
[6] M.A. Johnson, C.R. Webster and R N. Zare, J Chem. Phys 75 (1981) 5575.
[7] F. Bueso-Sanllehi, Phys Rev. 60 (1941) 556.
[8] M.A. Johnson, J. Rostas and R.N. Zare, Seventh Colloquium on High Resolution Molecular Spectroscopy, Reading, UK (1981)
[9] J. Rostas and R P. Tuckett, to be published.
[10] A. Carrington and R P. Tuckett, Chem. Phys Letters 74 (1980) 19.
[11] M. Heaven, T.A. Miller and V.E. Bondeybey, J. Chem. Phys. 76 (1982) 3831.
[12] P.C. Cosby and H. Helm, J. Chem. Phys. 76 (1982) 4720.
[13] R.D Brown, P.D. Godfrey, D.C. McGilvery and J.G. Crofts, Chem. Phys. Letters 84 (1981) 437.
[14] W. Demtröder, Laser spectroscopy (Springer, Berlin, 1981) p. 433.
[15] D. Gauyacq, C. Larcher and J. Rostas, Can. J. Phys. 57 (1979) 1634,
[16] J. Allison, T. Kondow and R N. Zare, Chem Phys Letters 64 (1979) 202
[17] E.W. Schlag, R. Frey, B. Gotchev, W.B. Platman and H Pollak, Chem Phys Letters 51 (1977) 406.
[18] J.P. Maier and F. Thommen, Chem. Phys. 51 (1980) 319.
[19] R C. Dunbar and D.W. Turner, Chem Phys. 57 (1981) 377.
[20] S. Gerstenkorn and P. Luc, Atlas du spectre d'absorption de la molécule d'iode (CNRS, Paris, 1978)
[21] D. Gauyacq, M. Horani, S. Leach and J. Rostas, Can. J. Phys. 53 (1975) 2040.
[22] M.A Johnson, J. Rostas, S. Leach and R.N. Zare, in preparation.
[23] M A. Johnson and J. Rostas, unpublished results.
[24] E.K C. Lee and G.L. Loper, in: Radiationless transitions, ed. S.H. Lin (Academic Press, New York, 1980) p. 1
[25] S Leach, M. Devoret and J.H.D. Eland, Chem. Phys. 33 (1978) 113.